Impact Simulation of Extreme Wind Generated Missiles on Radioactive Waste Storage Facilities

G. Barbella
Sogin S.p.A.
Via Torino 6 – 00184 Rome (Italy), barbella@sogin.it

Abstract: The structural design of temporary storage facilities for radioactive waste generally requires the fulfillment of highly severe performance criteria if compared to conventional buildings [1, 2, 4]. The present work focuses on the study of the behavior of a steel door subject to the impact of extreme wind generated missiles, which is one of the most demanding external events to account for. Two different kinds of scenario are considered: the first involves quasi-rigid small objects with limited mass and high translational velocity (hard impact); the latter involves massive objects with smaller velocity and larger contact areas (soft impact). Contact is here modeled both by imposing the non-penetration constraint in average terms, and by approximating the distribution of contact pressure over the impact area. Moreover, the nonlinear material behavior modeling allows one to account for the energy dissipation capabilities of the structure.

Keywords: contact, impact analysis, structural dynamics.

1. Introduction

The simulation of impact phenomena is one of the most challenging issues in the field of computational mechanics applied to engineering, mostly due to the rapid improvement of high-performance computing capabilities, as well as in the implementation of efficient numerical methods.

In the present work, the structural response of a steel door under impact loading is simulated. As above mentioned the effect of the collision with two different objects is studied: a circular steel tube and an automobile, representative of hard and soft impact respectively. The door structure is composed by a 10 mm thick steel panel with stiffening ribs and supported by a frame of UPN, HEA and IPE beams. All the parts are assembled with welded joints. A 3D view of the door structure is displayed in Figure 1, while Table 1 lists the main characteristics of the design missiles.

In the common practice the structural response is often evaluated by using approximated methods, based on simple models, and/or on the explicit definition of contact forces [2, 3]. However, these methods do not completely capture the evolution of the phenomenon and, in some cases, may lead to incorrect design choices. For these reasons, the evaluation of the mutual exchange of forces during the impact event should be determined by an explicit multi-body interaction analysis.

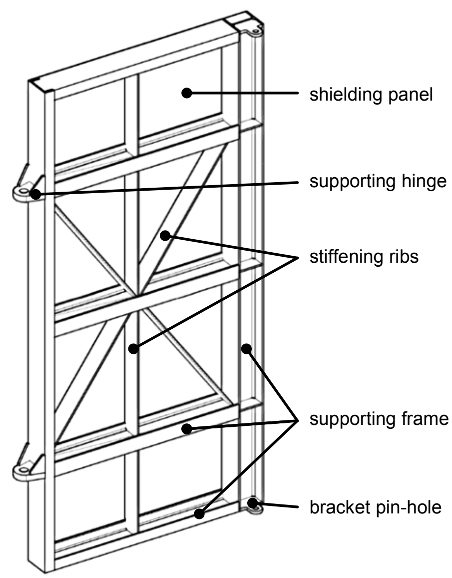

Figure 1. Back side 3D view of the single leaf of the steel door. The dimensions are 2.1 (width) × 4.0 m (height).

Table 1. Main characteristics of the missiles.

		automobile	steel tube
mass	[kg]	1000	35
velocity	[m/s]	12.25	24.5
kinetic energy	[kJ]	75	10.5
linear momentum	[kg m/s]	12250	857.5

The formulation of contact adopted in the present work, described in Section 2, is based on simple mapping tools directly implemented and available in Comsol Multiphysics. Provided that the shape and the extension of the interface area do not change during the impact event, or equivalently, that the variation of these characteristics is reasonably negligible, this approach guarantees reduced computational times if compared to classical contact formulations, since no search algorithm is required.

2. Model formulation

The numerical simulations are carried out by using Comsol Multiphysics Structural Mechanics and Nonlinear Structural Materials modules. Geometrical data of the door are acquired with the CAD Import module.

Both the impacting objects (target and missile) are explicitly included in the finite element models. In particular, solid, for 2D and 3D simulations, and shell elements, for 3D simulations only, are used.

Contact is here modeled exploiting the *general extrusion* tool under the model definition node of the Model Builder window. Let genext1 and genext2 be the mapping operators acting on the facing contact surfaces of the target and the missile respectively. Then, the expression

$$\Delta_{\mathrm{M}}(u) = u_{\mathrm{T}} - u_{\mathrm{M}} = u - \mathrm{genext2}(u), \qquad (1)$$

defined on the target surface, provides the difference between the values of the field variable u computed on the target and on the missile. Analogously, the same quantity can be evaluated on the missile impact surface as

$$\Delta_{\mathrm{T}}(u) = u_{\mathrm{T}} - u_{\mathrm{M}} = \mathrm{genext1}(u) - u . \qquad (2)$$

If u is the displacement component along the normal to the contact surface, eqs (1) and (2) provide the local gap distance between the impacting objects, denoted as d in the following.

The contact force per unit area is then expressed as a function of the gap distance and its time derivative:

$$F_{\mathrm{c}}(u,\dot{u}) = \left(k_{\mathrm{c}} d + c_{\mathrm{c}} \dot{d}\; h(\dot{d})\right) h(d), \qquad (3)$$

in which k_c and c_c are the elastic spring and the viscous damper penalty constants acting on the contact interface, while $h(x)$ is the unit step function centered in $x = 0$. It can be easily verified that F_c is non-null when $d > 0$, which defines the penetration condition of the impacting objects. Analogously, the viscous term is non-null when the penetration value is increasing.

As an alternative, when the impact area is small if compared to the characteristic structural dimension of the target, as in the case of the steel tube collision, one can consider the averaged values, over the contact area, of gap distance and gap velocity.

The formula in eq (3) is used within the Comsol model to define the boundary loads applied to the target and the missile surfaces, considering for the gap evaluation expressions (1) and (2) respectively. Friction effects are neglected in this study.

The penalty constants k_c and c_c have to be set in order to keep the penetration magnitude relatively small, and to avoid spurious high frequency vibrations which may arise due to local modes, generally related to the characteristic elements dimension.

The viscous constant is expressed in the following form:

$$c_{\mathrm{c}} = 2\,\xi \sqrt{k_{\mathrm{c}} m}\,, \qquad (4)$$

where ξ is the non-dimensional damping factor and m is the effective mass involved in the contact process. In this work, we conventionally set m equal to the total missile mass.

Dynamic equilibrium equations are solved via a step-by-step time integration algorithm based on second order backward difference formulas. This choice is recommended for two main reasons: first, the evolution of contact forces, which are frequently subject to large amplitude variations, needs extra robustness properties to be correctly captured and to avoid stability issues; secondly, the intrinsic numerical damping which characterizes this family of time integration schemes, can be useful to reduce the above mentioned spurious contributions related to the large value of the penalty stiffness constant.

3. Model validation

Validation tests were performed on a simplified 2D axisymmetric elastic model of a circular plate hit by a cylindrical hollow tube, having the properties listed in Table 1.

The diameter of the plate is 1 m and the thickness 10 mm, the external diameter of the tube is 76.2 mm (3 in) and a wall thickness of 6.8 mm is assumed. The clamped end condition at the boundary of the plate is simulated by concentrating a large mass (say almost infinite) at

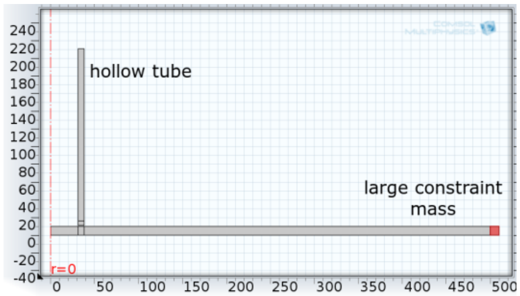

Figure 2. Geometry of the axisymmetric model of the circular plate (axes units are in mm).

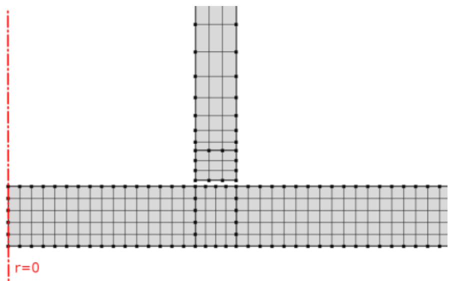

Figure 3. Particular of the mesh of the axisymmetric model.

the external border, as denoted in red in Figure 2. Contact forces are in this case averaged over the impact area. A particular of the mesh is shown in Figure 3. Finite elements with first order shape functions are adopted in the model.

The quality evaluation of the numerical results is carried out by monitoring the evolution of some key variables during the analyses, with the twofold objective to check the fulfillment of global energy and linear momentum balance principles, and to set the relevant parameters and tolerance thresholds of the solution algorithm.

Let consider the linear momentum balance principle applied to the missile body; one can write:

$$F_c(t) = \int_M \rho(\mathbf{x})\, a(\mathbf{x},t)\, \mathrm{d}V = \\ = \frac{\mathrm{d}}{\mathrm{d}t}\int_M \rho(\mathbf{x})\, v(\mathbf{x},t)\, \mathrm{d}V = \frac{\mathrm{d}}{\mathrm{d}t} P_M(t), \tag{5}$$

in which ρ is the mass density, a and v are the acceleration and velocity, and P_M is the linear momentum of the missile. The time histories of computed contact force and linear momentum derivative are compared in Figure 4, showing a perfect match during the impact event, even though some small discrepancies can be observed afterwards.

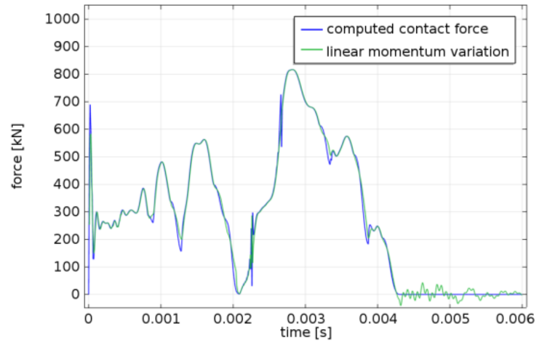

Figure 4. Axisymmetric model, comparison between the contact force and the variation of missile linear momentum.

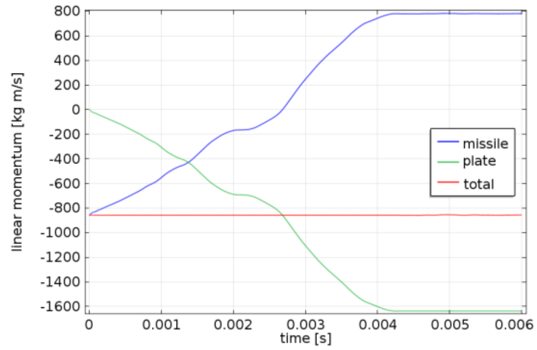

Figure 5. Axisymmetric model, comparison between missile and plate linear momentum.

Let now consider the whole system, including the missile and the plate: since external forces are null, the global momentum must be constant throughout the analysis, as it can be verified in Figure 5.

The curves of kinetic and strain energy of the system are displayed in Figure 6. The oscillations of total energy during the impact are due to

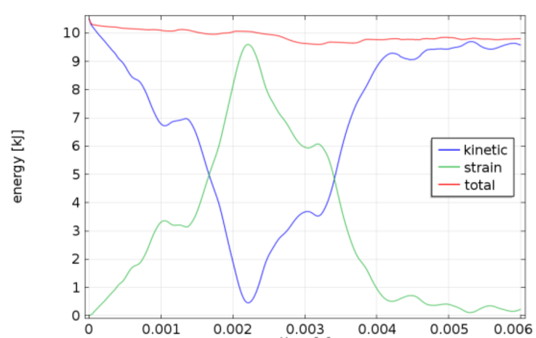

Figure 6. Axisymmetric model, time histories of kinetic and strain energy of the system.

the accumulation of strain energy in the contact spring layer, while a limited decrease can be noted comparing the final and initial values of total energy. Such a decrease, which is admissible in this context, is both due to the time integration scheme and to the contact penalty damper at the interface between the impacting objects.

Finally, it is worth noticing that the area under the computed contact force curve is considerably larger than the value of initial linear momentum of the steel tube. This is justified since the simulated impact is almost perfectly elastic, and the missile has a non-null rebound velocity after the collision, so that the time integral of the contact force is equal to the difference between the linear momentum computed after and before the collision.

4. Hard impact

The case of hard impact on the door is simulated by considering a local model of a single square frame of the shielding panel. This is justified since the fundamental period of the door, approximately 0.031 s, is much larger than the typical impact duration, meaning that the local response of the steel panel and the global response of the door structure can be reasonably considered as decoupled.

4.1. Model description

The size of the plate considered in the analysis is 780 × 780 mm, with a thickness of 10 mm. Analogously to what done in Section 3, the missile is modeled as an hollow tube having an external diameter of 3 in.

Exploiting the symmetries of the problem, both in terms of geometry and loading, one height of the square plate is modeled only, as shown in Figure 7. The mesh is refined towards the impact area at the center of the square, moreover, the discretization of the plate along the *z* axis is organized in layers, with elements of smaller thickness at the top and bottom faces. First order shape functions finite elements are adopted. An elastic-plastic constitutive law with Von Mises yielding function and isotropic hardening is assumed for the plate, while the missile material is considered as linear elastic, with the same elastic properties. Table 2 lists the relevant parameters used.

The contact penalty parameters used are:

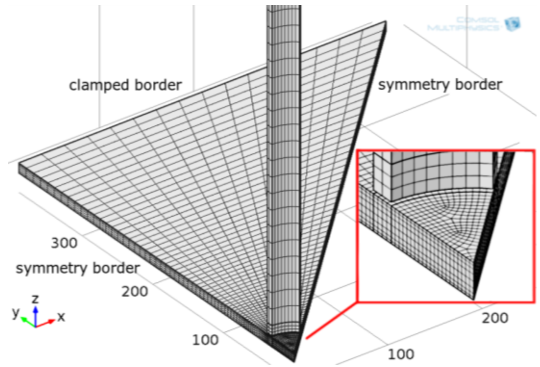

Figure 7. Square plate model, boundary conditions and mesh of the model.

$$k_c A_i = 5.0 \cdot 10^5 \text{ kN/m}, \quad \xi = 0, 1, \qquad (6)$$

A_i being the impact area.

Table 2. Material parameters adopted for the door steel panel.

parameter	symbol	value
Young modulus	E	210000 MPa
Poisson modulus	ν	0.3
initial yielding stress	$\sigma_{y,0}$	410 MPa
hardening modulus	E_{iso}	654 MPa

4.2. Results

The resulting contact force and displacement at the center of the plate are plotted in Figure 8, where the influence of the penalty damping is shown: if ξ = 1, high peak values of force are observed in the very first time instants, while a smaller damping ratio is more conservative. The duration and the shape of the force is similar to the curve obtained for the axisymmetric model of the circular plate. The maximum displacement, reached at the instant $t = 3$ ms, is 40 mm, with 33 mm of permanent deflection.

The development of plastic deformations is mostly localized in proximity of the impact area, at the opposite side with respect to the contact interface, as it can be seen in Figure 9. The maximum effective plastic strain is 14%, which is compatible with the characteristic failure parameters of the steel adopted, 20% being the minimum rupture elongation in a uniaxial test.

In this case, the resulting rebound velocity of the missile is about 6.1 m/s, meaning that during the impact the 94% of the kinetic energy possessed by the steel tube (9.85 kJ) is transferred to the plate.

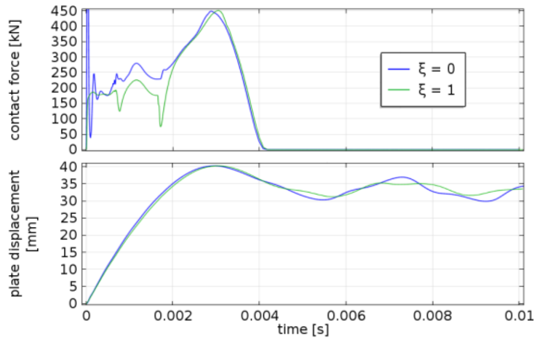

Figure 8. Square plate model, contact force and displacement time histories.

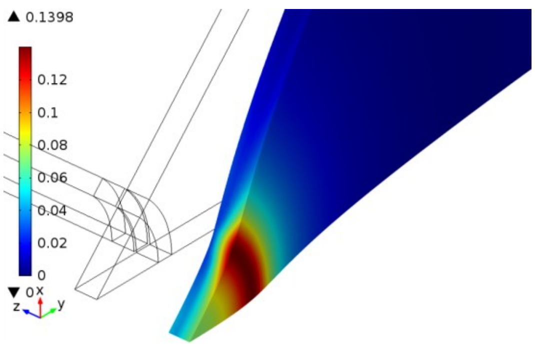

Figure 9. Square plate model, contour plot of effective plastic strain at the instant $t = 3$ ms, deformed shape is not amplified.

Simplified formulas to evaluate the permanent deflection and the time instant corresponding to the peak displacement of the plate may be taken from [5, 6 (§ 7.9.2)]. Under the hypothesis of a rigid-perfectly plastic material, the prediction for a fully clamped square plate hit by a rigid mass, substituting geometrical and material data, is: 26 mm of permanent displacement and peak value reached at ~ 2 ms. However, it has to be noticed that the accuracy of this approximation decreases if the ratio between the masses of the missile and the plate is small (~ 0.73), as in the present case.

The capability of a structure to dissipate energy is often evaluated by the so called push-over analysis, which provides the characteristic force-displacement curve, up to the failure of the system, determined by a maximum admissible ductility ratio.

Figure 10 displays the force-displacement curve obtained by applying an increasing uniform load to the impact area of the plate. The unloading phase starts from the maximum displacement computed in the dynamic contact simulation. Notice that, due to the boundary constraints, the structural response is influenced by membrane contributions from the very first steps of the test.

The area included within the loading and unloading curves, which is the energy dissipated in a quasi-steady cycle, is about 7 kJ. Therefore, in this case an equivalent static approach would have led to a larger demand of ductility.

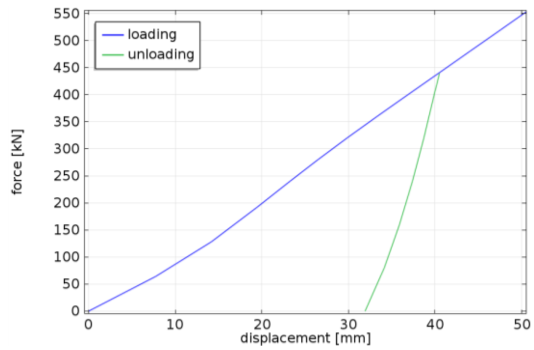

Figure 10. Pushover curve of the square plate. Force is applied to the impact area, control displacement is the maximum transverse deflection.

5. Soft impact

In the case of soft impact the analysis simulates the collision with an automobile having a mass of 1000 kg and a velocity of 12.25 m/s. Experimental data are available [2] showing that the impact of a typical automobile on a rigid wall produces a reaction force time history whose shape can be analytically approximated as

$$Q(t) = a\, m\, v_0 \sin(20t)\,, \tag{7}$$

defined within the interval $(0 : 0.025\,\pi)$ s, m and v_0 being the missile mass and initial velocity, while a is a coefficient, expressed in s^{-1}, such that the integral of the curve described by eq (7) is equal to the linear momentum $P = m\, v_0$ of the automobile. One obtains $a = 20\ s^{-1}$, therefore, the peak value of $Q(t)$ is 24.5 kN (mean value is 15.6 kN, corresponding to a mean deceleration of 15.9 g). This implies the assumption of a perfectly inelastic collision, meaning that both bodies have the same motion after the impact.

5.1. Missile calibration

In the present work, the missile is modeled as a solid block having the same global mass and velocity of the reference automobile. The dimensions of the block, in meters, are 1 × 1.6 × 4 ($H \times L \times P$), $H \times L$ being the impact area. The progressive damage of the automobile structures and the resulting internal dissipation of kinetic energy is globally reproduced by considering an elastic-plastic constitutive law with Von Mises yielding function and isotropic hardening. The mechanical characteristics of the material and the mass distribution are tuned, under the hypothesis of infinitely rigid target, in order to obtain a reaction force time history which approximately reproduces the curve $Q(t)$. The contact penalty parameters used in the simulations are:

$$k_c A_i = 5.0 \cdot 10^5 \text{ kN/m}, \quad \xi = 0. \tag{8}$$

The resulting mean values of peak penetration obtained in the tests do not exceed some tenth of millimeter, which is compatible with the infinitely rigid target constraint.

Several numerical tests were made to investigate the sensitivity of the model to the variation of each parameter. Table 3 lists the optimal combination of parameters identified by the tests for the material constitutive law; while the mass is distributed as follows: 97.5% of the mass is concentrated on the face opposite to the impact side, while the remaining 2.5% is uniformly distributed on the volume of the block.

Table 3. Material parameters adopted for the automobile solid model.

parameter	symbol	value
Young modulus	E	100000 kPa
Poisson modulus	ν	0.3
initial yielding stress	$\sigma_{y,0}$	4.9 kPa
hardening modulus	E_{iso}	500 kPa

As an example, Figures 11 and 12 show the influence of the mass distribution and the hardening modulus value on the shape and the duration of the contact force time history, in comparison with the target curve.

As noted in Section 3, the area under the curves of the computed contact force is still larger than the value of initial linear momentum of the automobile, even though to a lesser extent. In particular, in this case the rebound velocity is much smaller than the initial value. Such a condition is very close to, although moderately more conservative than the above stated hypothesis of perfectly inelastic collision at the basis of the analytic approximation in eq (7).

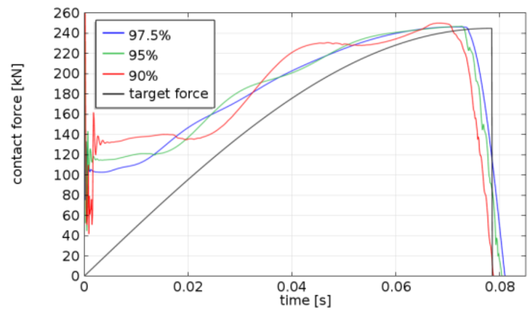

Figure 11. Missile model calibration, influence of mass distribution. The values in percent are referred to the amount of mass concentrated on the face opposite to the impact side.

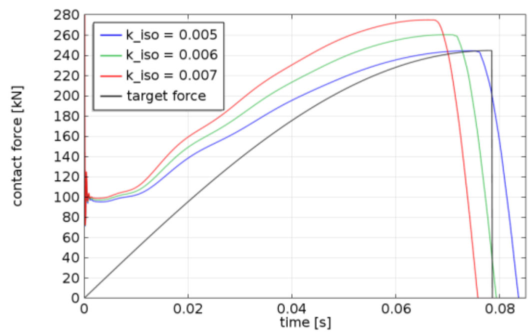

Figure 12. Missile model calibration, influence of isotropic hardening modulus, defined as $E_{iso} = k_{iso} E$.

5.2. Model description

As described in Section 1, the door structure is basically made of a supporting frame and a shielding panel. In the FE model, shell elements

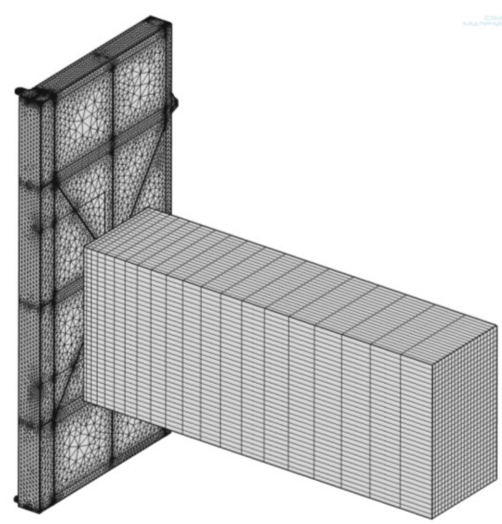

Figure 13. Door model, 3D view of the mesh including the missile.

are used for the latter, while all the remaining parts are discretized with solid elements.

The material properties of the missile are described above (see Section 5.1). As for the door structure, plastic behavior is assumed for the parts modeled with solid elements only, with $\sigma_{y,0} = 235$ MPa, and $E_{iso} = 235$ MPa, whilst the shielding panel is considered as linear elastic. This is justified because of the large value of initial yielding stress of the panel steel, meaning that no plastic deformations are expected for the automobile impact.

Contact forces are computed as a function of the local gap value, to account for the non-uniform distribution of pressure due to the rigidity of the different regions of the impact area.

5.3. Results

Figure 14 (top) shows the comparison between the computed contact force and the analytic approximation of eq (7). The dynamic interaction between the impacting objects has reduced the peak value of the force, increasing its duration. The maximum penetration observed over the contact interface is smaller than ~ 0.5 mm.

The transverse displacements of the door are reported in Figure 14 (bottom): the maximum values obtained by using the analytic input force and through an explicit impact simulation are similar. Moreover, reactions at the supports are reported in Figure 15: the use of eq (7) as input

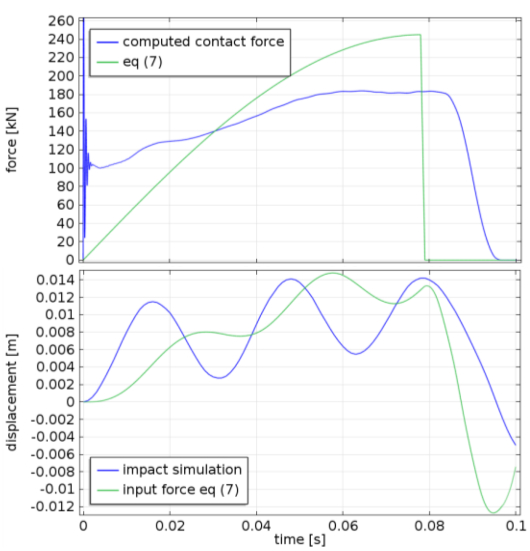

Figure 14. Door model, global contact force and maximum transverse displacement time histories.

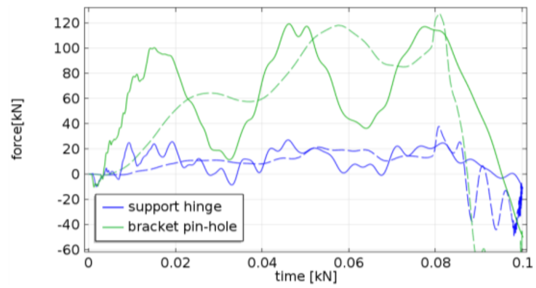

Figure 15. Door model, support reactions time histories, (solid lines) impact simulation, (dashed lines) input force eq (7).

force provides slightly larger peak values, while the results of the explicit impact analysis are characterized by a wider frequency content, meaning that this latter allows one to obtain a more accurate description of the phenomenon.

6. Conclusions

A procedure for the dynamic simulation of impact phenomena, within the Comsol Multiphysics framework, is presented and tested. The mutual exchange of contact forces between the impacting objects is explicitly modeled. Validation tests on a simple case are performed showing that linear momentum and energy balance principles are fulfilled. Moreover, a real-life example of a steel door under extreme wind generated missiles is analyzed and the results are shown, giving evidence that Comsol Multiphysics is a useful tool also for the dynamic simulation of impact problems.

7. References

1. ACI 349-06. Code Requirements for Nuclear Safety-Related Concrete Structures and Commentary, *American Concrete Institute* (2007)
2. BC TOP 9A Rev 02, Design of Structures for Missile Impact, *Bechtel Power Corporation* (1974)
3. Biggs J.M, Introduction to Structural Dynamics, *McGraw Hill* (1964)
4. DOE STD 3014-2006, Accident Analysis for Aircraft Crash into Hazardous Facilities, *U.S. Department of Energy* (2006)
5. Jones N, On the Mass Impact Loading of Ductile Plates, *Defence Science Journal*, **53**(1), 15−24 (2003)
6. Jones N, Structural Impact, 2nd edition, *Cambridge University Press* (2012)